Synthesis of Nanoscale $Ce_{1-x}Fe_xO_2$ Solid Solutions via a Low-Temperature Approach

Guangshe Li, Richard L. Smith, Jr., and Hiroshi Inomata*

Research Center of Supercritical Fluid Technology
Department of Chemical Engineering
Tohoku University, Sendai 980-8579, Japan

Received June 27, 2001

Synthesis of ceria-based solid solutions with controllable concentrations of oxygen vacancies and Ce^{3+} is of great fundamental significance because properties and applications of ceria-based solid solutions are determined by defect chemistry related to these concentrations, as well as effects from dopant size and valence.[1,2] Ceria shows much improved properties under doping.[1] The fluorite lattice is also capable of oxygen storage via electron flow between $Ce^{4+} \leftrightarrow Ce^{3+}$. Lower valence ions such as Pr^{3+} and Tb^{3+} in ceria influence the energetic properties by lowering the activation energy for oxygen migration,[3] while smaller ions such as Zr^{4+} enhance the oxygen storage capacity (OSC) by decreasing Ce^{4+}/Ce^{3+} reduction energy, preserving oxygen defects, and retarding OSC degradation at high temperatures.[4−6] Given the effects that low valence states and small ionic sizes have on properties[7] and defect reaction energies,[8] there could be considerable scientific and technological value for introducing undersized ions having lower valence into the ceria lattice and for identifying their role in defect chemistry. However, undersized lower valence ions such as Fe^{3+} are extremely difficult to dissolve into the ceria lattice by traditional methods. No solid solubility can be detected for Fe^{3+}-doped ceria sintered at 1200 °C.[9,10] In aqueous reflux systems, the main products are mixtures of goethite, hematite, and ceria. Here, we report on a synthesis route for $Ce_{1-x}Fe_xO_2$ solid solutions that occurs under mild conditions and produces nanoscale particles remarkably with a dopant content up to 15%.

Conventionally, nanosized oxides are prepared by solution chemistries,[11] among which sol−gel routes are frequently used.[11a,d,e] Precipitates obtained are typically amorphous with the particle surface being covered by a carbon residue that has to be removed by heat treatment.[11a] However, this treatment gives rise to surface contamination, particle agglomeration, and loss of the fine nature of the particles. Direct formation reactions are believed to decrease solid−solid interactions between particles during the calcination process.[12,13] Production of amorphous Ce−O networks from nitrate solutions occurs directly at low temperatures,[14] and is accompanied by release of nitrates via $Ce-O-NO_2$ on the sample surface and by subsequent formation of hydroxyl bonds via CeOH, with a net surface charge that is characteristic of metal oxide aqueous sols. By hydrothermal crystallization with NaOH as catalyst, it is possible that the relatively high electrostatic potential difference between the sols with surface charges can yield heterocoagulation of single phase products.[12c,15] Therefore, we adopted a hydrothermal method for $Ce_{1-x}Fe_xO_2$ to explore this synthesis route. Starting materials were $Ce(NO_3)_3 \cdot 4.4H_2O$ and $Fe(NO_3)_3 \cdot 9H_2O$. Solutions of 0.25 M $Ce(NO_3)_3$ and 0.25 M $Fe(NO_3)_3$ with Ce:Fe molar ratios from 95:5 to 70:30 were fully mixed for 2 h. A solution of 5 M NaOH was gradually added to the mixture with stirring. As the pH was increased above 8, a brown slurry appeared, which was determined to be amorphous. At a pH of 13, 10 cm^3 of slurry was transferred to 17 cm^3 Teflon-lined stainless steel autoclaves and reacted at 220 °C for 2 days. *Caution! Care must be taken to avoid overfilling autoclaves so that reactions occur at safe working pressures.* After cooling, samples were washed with distilled water until a pH of 7 and then air-dried at 50 °C.

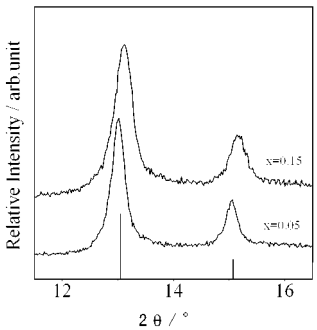

Figure 1. XRD patterns of typical samples of $Ce_{1-x}Fe_xO_2$ ($x = 0.05$, 0.15). Straight lines represent the standard data for ceria (JCPDS 34-394).

Elemental analysis of the samples by energy-dispersive X-ray spectrometry showed that the Ce:Fe molar ratios were close to the original solution molar ratios. Powder X-ray diffraction (Mo Kα radiation, $\lambda_{k\alpha 1} = 0.70932$ Å) indicated that when dopant content varied over a compositional range of 0.00 to 0.15, all diffraction peaks were highly symmetric and could be fitted as single peaks by a Lorentzian peak-shape function (Figure 1).

The broadening effect of the peaks can be attributed to the fine nature of the particles, which were 12 to 15 nm as calculated by Scherrer's formula. No traces of CeO_2, Fe_2O_3, $FeCeO_3$, or $FeCe_2O_4$ were observed, which indicates a different synthetic route from that of solid-state reactions where no solid solutions of $Ce_{1-x}Fe_xO_2$ are formed,[9] and from those of reduction reactions in the presence of metallic Fe or CO/CO_2 atmospheres where $FeCeO_3$ and $FeCe_2O_4$ are obtained.[16] Therefore, formation of cubic fluorite $Ce_{1-x}Fe_xO_2$ solid solutions was demonstrated. Compared with standard data for ceria, diffraction peaks for the solid solutions shifted systematically toward higher angles, corresponding to a lattice constraint that followed Vegard's law. This is

* Corresponding author. E-mail: inomata@scf.che.tohoku.ac.jp.

(1) (a) Park, S. D.; Vohs, J. M.; Gorte, R. J. *Nature* **1999**, *404*, 265. (b) Murray, E. P.; Tsai, T.; Barnett, S. A. *Nature* **1999**, *400*, 649.
(2) (a) Bamwenda, G. R.; Uesigi, T.; Abe, Y.; Sayama, K.; Arakawa, H. *Appl. Catal. A* **2001**, *205*, 117. (b) Chiodelli, G.; Flor, G.; Scagliotti, M. *Solid State Ionics* **1996**, *91*, 109.
(3) (a) Trovarelli, A. *Comments Inorg. Chem.* **1999**, *20*, 263. (b) Vidmar, P.; Fornasiero, P.; Kaspar, J.; Gubitosa, G.; Graziani, M. *J. Catal.* **1997**, *171*, 160.
(4) Balducci, G.; Kaspar, J.; Fornasiero, P.; Graziani, M.; Islam, M. S. *J. Phys. Chem. B* **1998**, *102*, 557.
(5) Hori, C. E.; Permana, H.; Simon, Ng K. Y.; Brenner, A.; More, K.; Rahmoeller, K. M.; Belton, D. *Appl. Catal. B* **1998**, *16*, 105.
(6) Mamontov, E.; Egami, T.; Brezny, R.; Koranne, M.; Tyagi, S. *J. Phys. Chem. B* **2000**, *104*, 11110.
(7) Li, P.; Chen, I. W.; Penner-Hahn, J. E. *J. Am. Ceram. Soc.* **1994**, *77*, 118.
(8) Minervini, L.; Zacate, M. D.; Grimes, R. W. *Solid State Ionics* **1999**, *116*, 339.
(9) Hrovat, M.; Holc, J.; Bernik, S.; Makovec, D. *Mater. Res. Bull.* **1998**, *33*, 1175.
(10) Tianshu, Z.; Hing, P.; Huang, H.; Kilner, J. *J. Mater. Proc. Technol.* **2001**, *113*, 463.
(11) (a) Liu, C.; Zou, B.; Rondinone, A. J.; Zhang, Z. J. *J. Am. Chem. Soc.* **2001**, *123*, 4344. (b) Rockerberger, J.; Scher, E. C.; Alivisatos, A. P. *J. Am. Chem. Soc.* **1999**, *121*, 11595. (c) Trentler, J. T.; Denler, T. E.; Bertone, J. F.; Agrawal, A.; Colvin, V. L. *J. Am. Chem. Soc.* **1999**, *121*, 1613. (d) Zarur, A.; Ying, J. Y. *Nature* **2000**, *403*, 65. (e) Feldmann, C.; Jungk, H. O. *Angew. Chem., Int. Ed.* **2001**, *40*, 359.
(12) (a) Wang, C. C.; Ying, J. Y. *Chem. Mater.* **1999**, *11*, 3113. (b) Turner, C. W. *Am. Ceram. Soc. Bull.* **1991**, *70*, 1487. (c) Ataie, A.; Piramoon, M. R.; Harris, I. R.; Ponton, C. B. *J. Mater. Sci.* **1995**, *30*, 5600.
(13) Adachi, G. Y.; Imanaka, N. *Chem. Rev.* **1998**, *98*, 1479.
(14) Nabavi, M.; Spalla, O.; Cakane, B. *J. Colloid Interface Sci.* **1993**, *160*, 459.
(15) Somiya, S.; Roy, R. *Bull. Mater. Sci.* **2000**, *23*, 453.
(16) (a) Belov, B. F.; Goroh, A. V.; Demchuk, V. P.; Dorschenko, N. A.; Somojlenko, Z. A. *Inorg. Mater.* **1983**, *19*, 231. (b) Robbins, M.; Wertheim, G. K.; Menth, A.; Sherwood, R. C. *J. Phys. Chem. Solids* **1969**, *30*, 1823.

10.1021/ja016502+ CCC: $20.00
Published on Web 10/11/2001

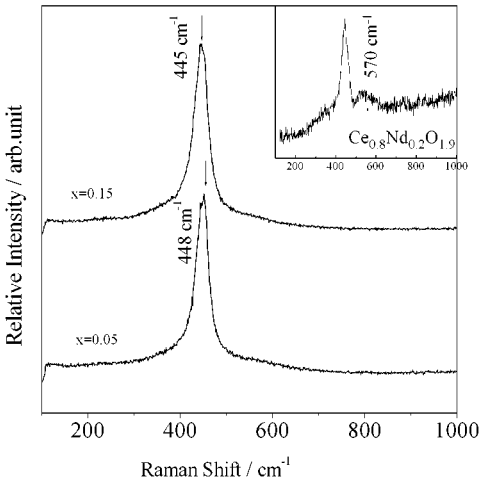

Figure 2. Raman spectra of $Ce_{1-x}Fe_xO_2$ ($x = 0.05, 0.15$). Inset: Raman spectrum of a sample of $Ce_{0.8}Nd_{0.2}O_{1.9}$ for illustrating the oxygen vacancy-related phonon mode at 570 cm^{-1}.

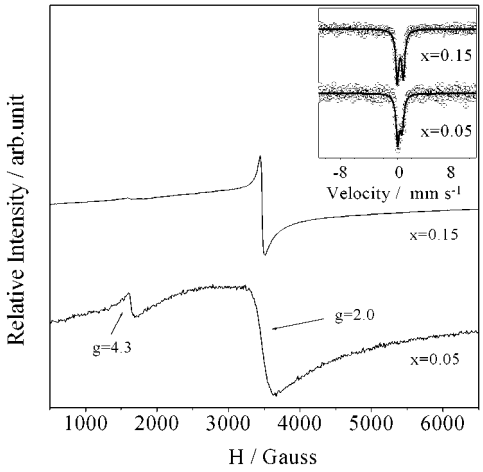

Figure 3. EPR spectra of $Ce_{1-x}Fe_xO_2$ ($x = 0.05,0.15$). Inset: Mössbauer spectra recorded at room temperature.

evidence for incorporation of Fe^{3+} in ceria on the basis of ionic size considerations. At a dopant level of $x = 0.20$, a second phase of hematite Fe_2O_3 appeared, which probably occurred due to diffusion of the Fe^{3+} from the bulk to the sample surface.

Oxygen vacancies in $Ce_{1-x}Fe_xO_2$ were monitored by Raman spectroscopy. Figure 2 shows Raman spectra for typical samples of $Ce_{1-x}Fe_xO_2$ ($x = 0.05, 0.15$), and that of $Ce_{0.8}Nd_{0.2}O_{1.9}$ for comparison (inset). The phonon mode at 570 cm^{-1} is characteristic of oxygen vacancies in the ceria lattice,[17] as is clearly seen in the inset. However, no phonon mode was observed at 570 cm^{-1}, which shows an extremely low concentration of oxygen vacancies. The intensive phonon mode observed at ca. 440 cm^{-1} can be assigned to the symmetric breathing mode of oxygen atoms around the cerium ions.[18] This mode was ca. 30 cm^{-1} lower than the literature value of 470 cm^{-1} for undoped ceria,[17] which can be explained by the enlarged Ce−O bond lengths resulting from lattice distortions.

Valence states of Ce in $Ce_{1-x}Fe_xO_2$ solid solutions were determined by electron paramagnetic resonance (EPR). No characteristic signals of Ce^{3+} were observed at $g = 1.96$ and 1.94,[19] in Figure 3, indicating that $Ce_{1-x}Fe_xO_2$ was essentially free of Ce^{3+}. Two EPR signals observed at $g = 4.3$ and 2.0 are associated with the $Fe^{3+}O_6$ unit having distorted rhombic symmetry.[20] This was confirmed by Mössbauer spectra (inset) that showed a paramagnetic doublet with hyperfine parameters (vs α-Fe) of 0.38 and 0.78 mm/s for isomer shift and quadrupole splitting, respectively, which are characteristic of high-spin Fe^{3+} in a distorted octahedral site.[21]

A structural model associated with defect chemistry can be proposed to explain the absence of oxygen vacancies and Ce^{3+} in $Ce_{1-x}Fe_xO_2$. Since Fe^{3+} has a much smaller ionic size compared with the host Ce^{4+}, it can occupy either network Ce^{4+} sites or interstitial sites in the fluorite lattice.[8,22] When Fe^{3+} becomes substituted at the Ce^{4+} sites, oxygen vacancies are essential for the charge balance, while for the case of interstitial Fe^{3+}, excess oxygen species can be expected. In the ceria lattice, oxide species can hop readily through passages near interstitial sites due to the relatively smaller energy barriers. In the formation of $Ce_{1-x}Fe_xO_2$, Fe^{3+} becomes substituted at a Ce^{4+} site and an interstitial site. The interstitial oxygen species associated with the interstitial Fe^{3+} diffuse to adjacent oxygen vacancies associated with Fe^{3+} at the Ce^{4+} site, giving rise to an extremely low concentration of oxygen vacancies according to the probable defect reaction of the pairs, $3Fe_{Ce}'/Fe_i'''$. Therefore, the large amount of interstitial Fe^{3+} must be the primary reason for the increased lattice constraint and lattice distortion, as observed by the Raman measurements. These factors bring about an increased barrier for electrons moving between Ce^{3+} and Ce^{4+}, and play an important role in adjusting the reduction equilibrium in the ceria lattice.

In summary, nanoscale $Ce_{1-x}Fe_xO_2$ solid solutions with a high Fe^{3+} content have been synthesized by a low-temperature approach. High-spin Fe^{3+} appeared to be distributed at Ce^{4+} and interstitial sites according to a ratio of ca. 3:1, which accounted for the extremely low oxygen vacancy concentration and the absence of Ce^{3+}. Finally, there is a possibility of increasing the relative content of Ce^{3+} in these solid solutions, if extra free oxygen vacancies can be introduced by co-doping with oversized dopants such as Bi^{3+} as described in ref 23.

Acknowledgment. The authors are grateful to the following Tohoku University faculty for assistance: Dr. H. Onodera, Mössbauer spectra; Dr. M. W. Watanabe, EPR/Raman spectra; and Prof. T. Endo and Dr. H. Takizawa, EDX. Financial support was provided by Monbusho general funds and a postdoctoral fellowship.

JA016502+

(17) Mineshige, A.; Taji, T.; Moroi, Y.; Kobune, M.; Fujii, S.; Nishi, N.; Inaba, M.; Ogumi, Z. *Solid State Ionics* **2000**, *135*, 481.
(18) McBride, J. R.; Hass, K. C.; Poindexter, B. D.; Weber, W. H. *J. Appl. Phys.* **1994**, *76*, 2435.
(19) Sergent, N.; Lamonier, J. F.; Aboukais, A. *Chem. Mater.* **2000**, *12*, 3830.
(20) (a) Griffith, J. S. *Mol. Phys.* **1964**, *8*, 213. (b) Li, L.; Li, G.; Smith, R. L., Jr.; Inomata, H. *Chem. Mater.* **2000**, *12*, 3705.
(21) Takano, Y.; Okada, T.; Nakagawa, S.; Suzuki, H.; Matsumoto, T.; Noro, S.; Yamadaya, T. *Mater. Res. Bull.* **1995**, *30*, 789.
(22) Hoffman, A.; Fischer, W. A. *Z. Phys. Chem. NF* **1958**, *17*, 30.
(23) Li, G.; Mao, Y.; Li, L.; Feng, S.; Wang, M.; Yao, X. *Chem. Mater.* **1999**, *11*, 1259.